Progress In Electromagnetics Research M, Vol. 78, 83–92, 2019

Investigations of Specific Absorption Rate and Temperature Variations for an UWB Antenna for Wireless Applications

Mohandoss Susila, Thipparaju Rama Rao*, Karthik Varshini, Palaniswamy Sandeep Kumar, and Marudappa Pushpalatha

Abstract—This paper portrays a compact planar ultra-wideband (UWB) antenna design and development for wireless applications. The proposed antenna is influenced by fractal geometry design, where a pentagon slot is introduced inside a circular metallic patch, and iterations were carried out to achieve needed wide bandwidth. The antenna is deployed over an FR4 substrate with relative permittivity of 4.4 and thickness of 0.16 cm, to achieve wider impedance bandwidth. The proposed antenna is of low profile with dimensions of 32×32 mm, and it operates over bandwidth of 12.1 GHz (2.9–15 GHz). Specific Absorption Rate (SAR), the measure of exposure of electromagnetic (EM) energy on human tissues, is observed when proposed antenna is placed in close proximity to the dispersive phantom model. Also, the time domain analysis is done on human tissue model to observe the performance of the antenna and to validate its capability with wireless devices which are in near vicinity to the human all the time. Further, in this research, the temperature variation on human tissue is examined using Infrared (IR) thermal camera. Investigation on these parameters and validation with Radio Frequency (RF) equipment helps to prove that the proposed antenna is a suitable candidate for UWB wireless communication applications.

1. INTRODUCTION

The prospects of short-range wireless communications over globe are brightening at greater heights, where wireless devices communicate with each other at short distances for exchange of multimedia content. Human will be a carriage of these devices which are capable of operating in various bands based on the applications. For any devices to communicate, antenna is one of the important entities, whose design is of very much importance for its compactness, low cost, easy fabrication, easy integration with other electronic modules and also multi-functional use. This has created interest among the researchers to explore this field. Designing an antenna to the desired wide band of frequency range and meeting the desired objectives to operate for short-range communications is one of the challenging tasks. The Specific Absorption Rate (SAR) has its significance where the electromagnetic (EM) waves from the antenna are exposed to the human body for a short term or longer period of time. Further, the SAR analysis and thermal effect gives a detailed report of the antenna and its applicability when it is placed in close proximity to human. A number of researches have been done in designing an antenna, which is examined for its SAR and temperature variations.

After the release of UWB spectrum for commercialization by FCC [1], many works have aimed at designing the antenna operating over the entire band because of its widespread applications in the field of medical, personal communications, vehicular, radar and other short-range communications. In [2] the authors proposed a low profile pentagonal antenna that operated over a wideband designed for wearable applications. Authors in [3] designed a reconfigurable spiral antenna for biomedical applications over

Received 16 November 2018, Accepted 16 January 2019, Scheduled 24 January 2019
* Corresponding author: Thipparaju Rama Rao (ramaraotr@gmail.com).
The authors are with the SRM Institute of Science and Technology, Kattankulathur, Chennai 603203, India.

an FR4 substrate with a size of $32 \times 50.3 \times 1.8\,\text{mm}^3$. In a Q-slot monopole antenna for UWB body centric communication, a slot was introduced in the patch to have additional resonance [4]. Paper [5] discussed the bandwidth enhancement technique and also addressed SAR issues using T-junction dual symmetrical meander line antenna. A detailed study was carried on the performance of the antenna due to change in the thickness of the outer layer of human tissue. In [6], the authors presented an extensive study regarding the effect of different tissue thicknesses on the UWB antenna performance by simulations with a parametric layered human body tissue model. In [7], Ray proposed various configurations of monopole antennas and discussed their performances for UWB applications. In [8], the authors analyzed SAR in different parts of the body using infrared thermography, and in [9, 10], the thermal distributions over the body were investigated for wearable wireless applications.

In this research, a planar monopole antenna is presented adopting the fractal geometry using a simple configuration of circle and pentagon. Modification of ground plane is done by tapering and introducing slits in it as well creating a slot (U-shaped) in the feed line for the enhancement of the impedance bandwidth and gain. The proposed antenna is studied for its radiation properties and impedance bandwidth. In this work, the time domain analysis is carried out to examine the antenna's behavior in free space and proximity to human body. The main emphasis is on SAR on the three layered human tissue model and the temperature variation on the human body when being exposed to short term EM radiation. Further, the temperature elevation is examined by infrared (IR) thermography technique using IR thermal camera.

The flow of the present work is discussed as follows. Section 1 provides the introduction about the work and related similar works. Section 2 presents the design of antenna and its characteristics in terms of reflection coefficient and radiation pattern. Section 3 discusses the study of time domain analysis that is carried out in free space and on-body. Investigations of SAR and temperature elevation of the body tissue when the antenna is in close proximity to the human body is discussed in Section 4, and the last section concludes the work.

2. ANTENNA DESIGN CONFIGURATION AND ITS PERFORMANCE ANALYSIS

The proposed antenna is designed using Ansys — High Frequency Structure Simulator tool. The antenna is derived using a simple configuration of circle and pentagon on an FR4 epoxy substrate of 4.4 relative permittivity, 0.02 loss tangent, and 1.6 mm thickness. The dimension details of the proposed antenna are represented in Fig. 1, in which R_1, R_2, R_3 and R_4 are the radii of the 0th, 1st, 2nd, and 3rd iterations to cover the entire UWB. Similarly, the sides of the pentagon are taken as per the circle radius so that the ratio is maintained in order to fit inside the corresponding circles, and its values are listed in Table 1. The partial rectangular ground plane of $32\,\text{mm} \times 12\,\text{mm}$ is tapered along the sides, and a few slits are introduced on the top of the ground plane to enhance the desired impedance bandwidth characteristics. The overall dimension of the antenna is $32 \times 32 \times 1.6\,\text{mm}^3$, and the scale factor for each iteration is maintained constant. It is given as follows,

$$\frac{R_1}{R_2} = \frac{R_2}{R_3} = \frac{R_3}{R_4} = 1.3 = \frac{P_1}{P_2} = \frac{P_2}{P_3} = \frac{P_3}{P_4} \tag{1}$$

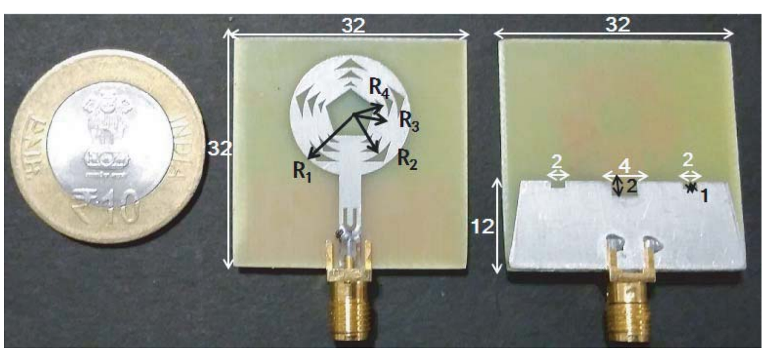

Figure 1. Photograph of the Prototype with dimensional details. (Dimensions are in mm).

Table 1. Dimensional details.

Iteration (i)	Circle Radius (R_i)	Pentagon Sides (P_i)
1	8.5	9.52
2	6.7	7.52
3	5.3	5.64
4	4.1	4.35

The antenna construction with parametric analysis is detailed in [11]. The performance of the antenna over its operating band is examined by measuring the reflection coefficient and radiation pattern. Anritsu MS2073C vector network analyzer is utilized for experimentation purpose. After proper calibration, the prototype of the proposed antenna is tested for its performance. The measured reflection coefficient is plotted and compared with the simulated result, which is illustrated in Fig. 2. It is evident that the impedance bandwidth matches simulated output. The variation in frequency dips at higher frequencies is due to cable loss and the lossy nature of substrate FR4 at higher frequencies. The measured radiation pattern along E-plane and H-plane for frequencies 3.1, 6.8 and 10.6 GHz are presented in Fig. 3. From the radiation pattern, it is seen that the antenna maintains omnidirectional pattern in the H-pane and directional in the E-plane. At higher frequencies, there are slight pattern disturbances due

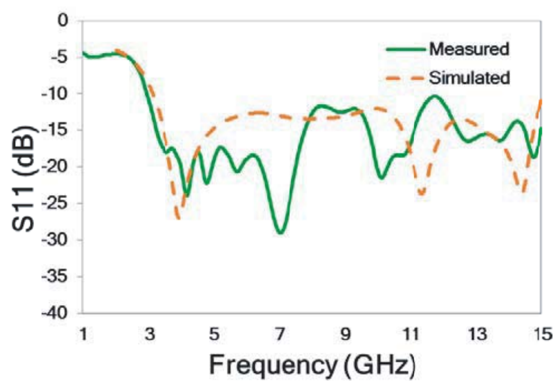

Figure 2. Measured and simulated reflection coefficient of the proposed antenna.

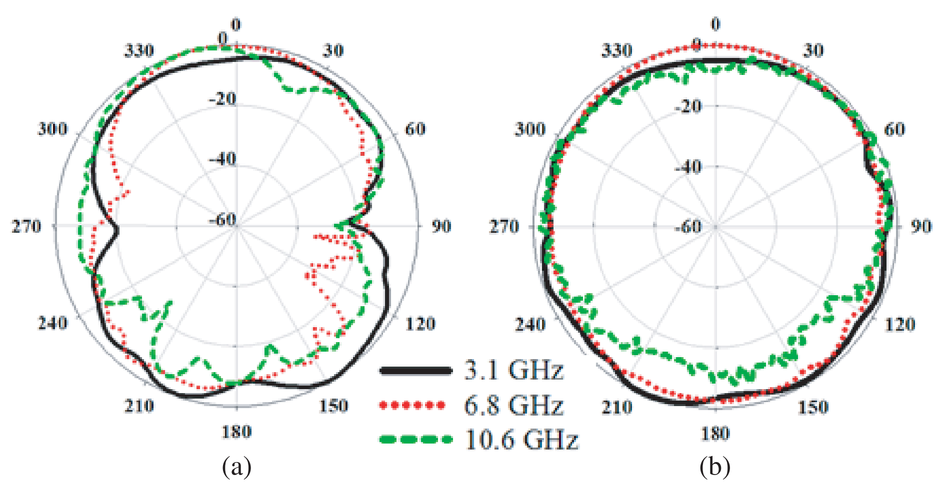

Figure 3. Measured radiation pattern of the proposed antenna (a) E-plane, (b) H-plane at 3.1, 6.8 and 10.6 GHz.

to lossy nature of the substrate. The proposed antenna is nearly omnidirectional over the frequency band. The time domain analysis of the proposed antenna is described in [11]. The antenna is validated for its performance over the operating band, by time domain analysis in free space and in close vicinity to the body, which is discussed in next section.

3. TIME DOMAIN ANALYSIS OF THE ANTENNA WHEN PLACED IN CLOSE PROXIMITY TO THE BODY

Time domain analysis is carried out to examine and validate the antenna by the parameters like S_{21}, group delay for its suitability to operate in UWB band [12, 13]. S_{21} is measured to validate its constant magnitude and phase linearity over the operating frequency band. Group delay is a measure of phase distortion of the signal. Time domain analysis of the antenna describes the performance of the antenna in a detailed manner. A brief analysis is carried out in time domain, to observe the performance of antenna when placed in proximity to the three layer human tissue model and in free space. The parameters such as magnitude and phase of S_{21} and group delay are investigated. The two identical antennas are placed 5 mm above the tissue layer with 200 mm separation between them. The tissue properties and dimension are taken as shown in Fig. 4, and it conveys the front and top views of the arrangement of antenna placed in close proximity to the human tissue model for time domain analysis.

Transfer function of a system relates the characteristics of transmitter, receiver and the propagation channel, which can be studied through S_{21}. The magnitude and phase of S_{21} in free space and in close proximity to the body are depicted in Fig. 5 and Fig. 6, respectively. It is observed that the phase

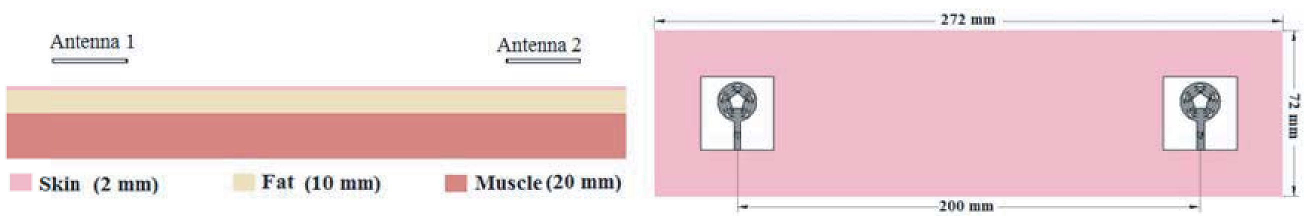

Figure 4. Three layered human tissue model for time domain analysis with identical antenna placed side by side place at a distance of 5 mm from the skin (Front and Top view).

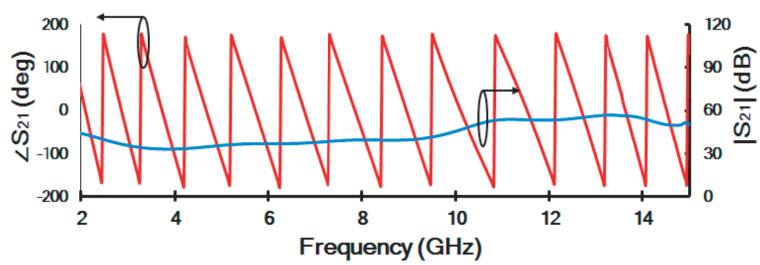

Figure 5. Magnitude and phase of S_{21} for antenna placed side by side in free space.

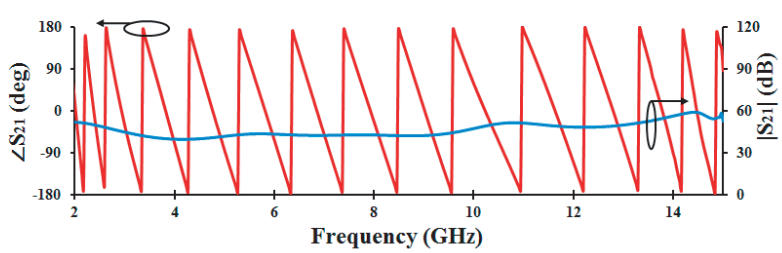

Figure 6. Magnitude and phase of S_{21} for antenna placed side by side on hand.

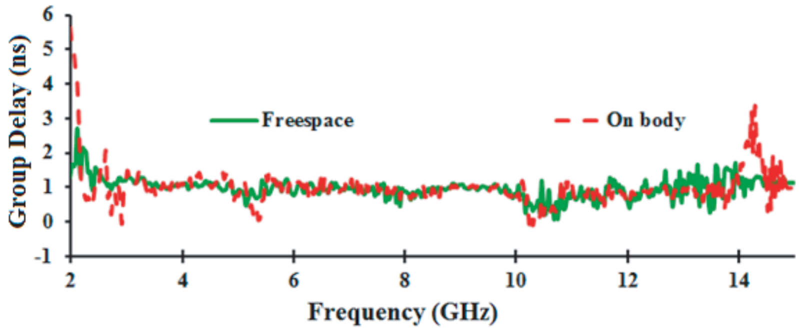

Figure 7. Group delay of the antenna in free space and in close proximity to the body.

is linear, and it maintains almost constant magnitude in free space and also in close proximity to the body. Group delay of the antenna in free space and in near proximity to the body is shown in Fig. 7, and it is observed to be less than 1.5 ns.

4. INVESTIGATIONS OF SAR AND THERMAL EFFECT

4.1. Investigations of Specific Absorption Rate

SAR is the measure of absorption of EM energy by human body, and it is validated for human exposure to EM energy below the prescribed limit of 1.6 W/kg over 1 g of tissue [14] and 2 W/kg over 10 g of tissue [15]. In this research work, the SAR value is calculated for the proposed antenna when it is in proximity to the body. SAR analysis is carried over a three layered model of human tissues with size 100 mm × 100 mm. The SAR is calculated on different locations of the body considering the corresponding thicknesses of muscle, fat, and skin [16]. The antenna is placed at a distance of 5 mm from the three layered tissue model as shown in Fig. 8, depicting that the antenna is placed in close proximity to the body. Table 2 shows the tissue properties of the three layered body tissue. The dispersive tissue properties are selected for the three layers as per the literature [16] and listed in Table 3 for three different frequencies: 3.1, 6.8 and 10.6 GHz in terms of dielectric constant, conductivity, loss tangent, penetration depth, and wavelength. It is observed from Table 3 that the penetration depth for all the tissues decreases as the frequency increases. SAR depends on the geometry, size, and orientation of the exposed subject, incident field intensity, frequency and also the exposure time. SAR is defined as a function of inducted electric field (E, V/m), electrical conductivity (σ, S/m), and mass density of the

Table 2. Human body tissue properties.

Tissue	Mass density (kg/m^3)	Heat Capacity (J/kgK)	Thermal Conductivity (W/m/K)
Skin	1100	3.5	0.293
Fat	910	2.5	0.201
Muscle	1041	3.546	0.53

Figure 8. Three layered tissue model.

Table 3. Dielectric properties of human tissue model @ 3.1, 6.8 and 10.6 GHz.

Tissue Layer	Frequency (GHz)	Relative Permittivity	Loss Tangent	Conductivity (S/m)	Penetration Depth (m)	Wavelength (m)
Skin	3.1	37.358	0.2786	1.7949	0.018249	0.015674
	6.8	34.215	0.3584	4.6731	0.006748	0.007368
	10.6	30.705	0.4806	8.7019	0.003472	0.004969
Fat	3.1	5.2138	0.15011	0.13497	0.090060	0.042235
	6.8	4.8608	0.19612	0.36327	0.032372	0.019757
	10.6	4.5572	0.23373	0.62812	0.018164	0.013160
Muscle	3.1	51.936	0.24804	2.2216	0.017351	0.013319
	6.8	47.069	0.34935	6.2663	0.005898	0.006287
	10.6	41.954	0.46476	11.498	0.003066	0.004258

tissue (ρ_m, kg/m^3) and is calculated by Equation (2).

$$SAR = \sigma \frac{|E|^2}{\rho_m} \tag{2}$$

The depth of penetration (δ, m) of EM waves to the tissues exposed depends on the electrical properties of the tissue and the frequency of the source, which are related by Equation (3), where σ is the electrical conductivity of tissue (S/m), μ the magnetic permeability of the tissue (H/m), and f the frequency of operation (Hz).

$$\delta = \sqrt{\frac{1}{\pi \mu \sigma f}} \tag{3}$$

Thermal effects for short term exposures are measured using infrared thermography to investigate the temperature elevation of the body. Also, the rise in temperature is found in compliant with international safety regulations (safety exposure guidelines of 1°C), preferring the use of the antenna for wireless applications. Table 4 lists the SAR, on the typical three layered tissue model with the thicknesses of skin, fat, and muscle. The SAR is investigated in different locations of the body such as forehead, forearm, chest, abdomen, and thigh where the thicknesses of skin, fat, and muscle are different. SARs for 1 g of tissue in different locations of the body are listed in Table 4, and it is noted that the SAR is high on the skin layer. It is observed that the SAR value is comparatively much less than the specified limits, preferring the proposed antenna for its suitability to short range UWB wireless communications. Further, the thermal effect on the body for short term EM exposure through the antenna is investigated in the next section.

4.2. Investigation of Thermal Effect On-Body

Radiation dosimetry in the field of radiation protection is the measurement, calculation and assessment of the dose of ionized radiation absorbed by human body [15]. Heating is the major effect in the range of frequencies from 10 MHz to 300 GHz due to the absorption of EM energy, and rise in temperature exceeding 1–2°C will cause adverse effects on human [10]. IR thermography is one of the techniques used to study the thermal effect of the body when antenna is in close proximity to the body. Using this technique, the thermal effect is measured when the handheld device or excited antenna is placed in close proximity to the body for a long duration.

For UWB applications, all devices are handled with low power, but the exposure of the antenna for long duration leads to some temperature rise on the human body due to thermal effect. To measure the temperature elevation, the proposed antenna is placed over the right forearm and is excited for a short term of 20 minutes. The experimental setup for assessing the surface temperature elevation due to EM exposure from the antenna prototype is represented in Fig. 9 with sample thermograms. The entire

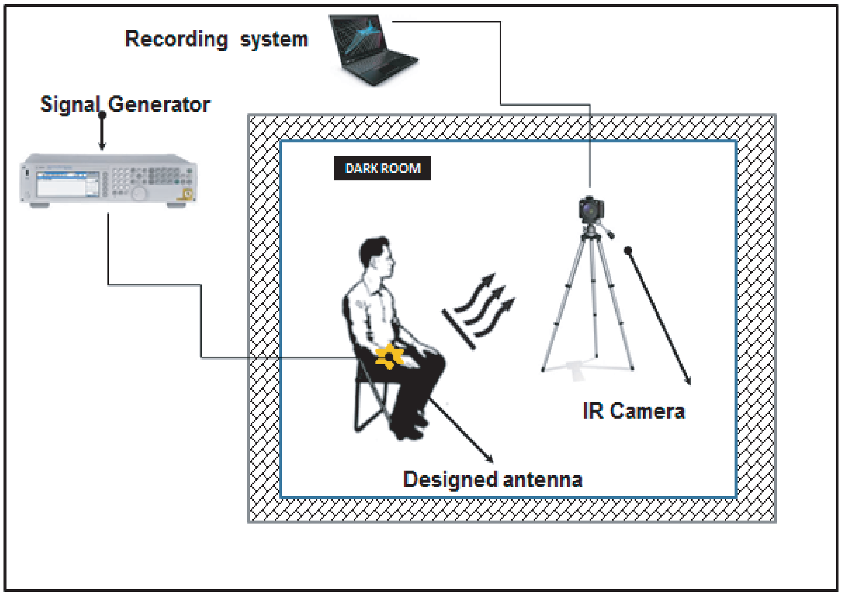

(i)

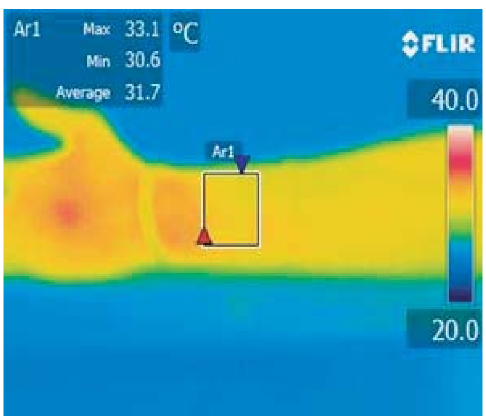

(a)

(ii)

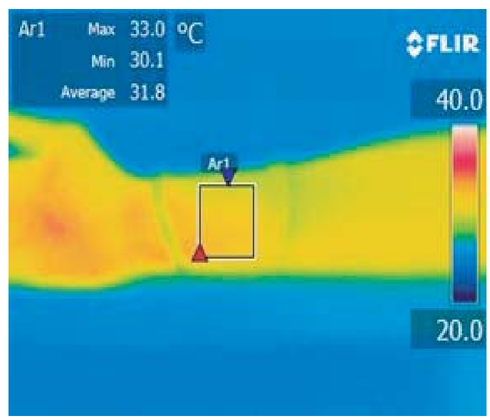

(b)

Figure 9. Temperature variations for short term EM exposure: (i) Experimental setup and (ii) Sample thermogram: (a) at 0 minute and (b) 20 minutes taken on the right forearm at 6 GHz.

measurement is done in the research lab, located on 13th floor of our university. During measurement, precautionary measures such as disconnecting Wi-Fi and interfering devices (our mobile phones) are kept out of the measurement area and also with all the lights switched off. Due to measurement constraints and equipment availability, the thermal effect is calculated for different frequencies up to 6 GHz at 1 mW input power fed through Anritsu MS2830A vector signal generator. Thermograms were taken at 0 minute (assumed as initial condition) and after 20 minutes of RF exposure continuously. Sample thermograms are presented in Fig. 9 which depicts the temperature variations for short term exposure for 6 GHz. Table 5 lists the temperature variations for different frequencies at 3.1 and 6 GHz, due to measurement capability.

Thermal effects for short term EM exposures are measured using IR thermography to investigate the temperature elevation of the body. Also, the rise in temperature is found in compliant with international safety regulations (safety exposure guidelines of 1°C), preferring the use of the antenna for wireless applications. The proposed antenna is compared with similar works available in the literature, in terms of size, operating band, and SAR which are specified in Table 6. From the table it is evident that the antenna size is compact, and it has wide bandwidth preferring it for wireless applications.

Table 4. SAR values for different layers in different locations of the body for 1 g of tissue at 3.1, 6.8 and 10.6 GHz.

Different locations on the body	Tissue	Thickness (mm)	SAR_{1g}		
			3.1 GHz	**6.8 GHz**	**10.6 GHz**
Forehead	Skin	1.06	0.08910	0.14032	0.06974
	Fat	3.06	0.01525	0.02123	0.01490
	Muscle	10	0.20328	0.08873	0.03114
Forearm	Skin	0.61	0.02650	0.07117	0.06228
	Fat	0.90	0.00308	0.00452	0.00386
	Muscle	10	0.18207	0.13091	0.06519
Chest	Skin	2.01	0.14987	0.07678	0.06529
	Fat	3.10	0.01164	0.00845	0.00997
	Muscle	10	0.16589	0.03512	0.02228
Abdomen	Skin	2.3	0.17530	0.06495	0.08806
	Fat	10	0.03120	0.04670	0.03355
	Muscle	20	0.04690	0.03326	0.01552
Thigh	Skin	1.86	0.19930	0.06456	0.06456
	Fat	5.61	0.02346	0.01712	0.03102
	Muscle	10	0.11715	0.02439	0.02763

Table 5. Temperature values from Thermograms for different frequencies at 0 and 20 minutes.

Frequency (GHz)	Thermogram (°C)		
	Initial 0 seconds	**After 20 min**	**Temperature Elevation**
3.1	28.9	29	0.1
6	31.7	31.8	0.1

Table 6. Comparison of proposed work with existing similar antennas.

Ref.	Substrate	Freq. Range (GHz)	Size (mm^3)	SAR
[17]	FR-4	0.4, 2.4–2.5	$32 \times 50.3 \times 1.8$	NA
[18]	FR-4	2.9–11	$15 \times 25 \times 1.6$	**GHz** **3.1** **6** **10.5** Skin 8.35 220 110 Fat 38.8 1.7 8.3 Muscle 25.5 56.9 8.6 (5 mm above the body — SAR mW/kg)
[19]	FR-4	3.3–12	$36.6 \times 39 \times 1.6$	38.1 W/kg @ 9 GHz (3 mm above the body)
[20]	FR-4	2.4–2.7	$30 \times 40 \times 1.6$	0.98 W/kg @ 2.5 GHz (15 mm above the body)
Proposed Antenna	**FR4**	**2.9–15**	$32 \times 32 \times 1.6$	**GHz** **3.1** **6.8** **10.6** Skin 30 70 60 Fat 3 4 3 Muscle 182 130 65 (5 mm above the body — SAR mW/kg)

5. CONCLUSIONS

A UWB based planar monopole antenna is developed for short-range wireless applications. The observed impedance bandwidth of 12.1 GHz (between 2.9 and 15 GHz) maintaining almost omnidirectional pattern over the desired band. The simulated results of wide bandwidth and radiation characteristics agree with measured values. The performance analysis of the proposed antenna in frequency and time domain analysis concludes that it is well suited for UWB wireless applications as S_{21} is maintained with linear phase and almost constant magnitude, and the group delay is well below 1.5 ns. The designed antenna is investigated for SAR and thermal effect due to the EM exposure when the antenna is kept in close proximity to the human body. Further, the temperature elevation due to the short term EM exposure is also examined with the help of IR camera experiments and is found around 0.1°C. From the study, it is evident that the SAR values are well below the limit specified by the FCC and other safety regulations, making the proposed antenna a good candidate for short-range wireless applications which are proliferating in a big way.

ACKNOWLEDGMENT

The authors are very much thankful to the DRDO, Govt. of India for their executional support.

REFERENCES

1. Tuovinen, T., M. Berg, K. Y. Yazdandoost, and J. Iinatti, "Ultra wideband loop antenna on contact with human body tissues," *IET Microwaves, Antennas & Propagation*, Vol. 7, No. 7, 588–596, 2013.
2. Doddipalli, S., A. Kothari, and P. Peshwe, "A low profile ultrawide band monopole antenna for wearable applications," *International Journal of Antennas and Propagation*, Vol. 2017, Article ID 7362431, 9 pages, 2017.
3. Sali, M. and A. Pourziad, "A novel reconfigurable spiral-shaped monopole antenna for biomedical applications," *Progress In Electromagnetics Research Letters*, Vol. 57, 79–84, 2015.
4. Yeboah-Akowuah, B., P. Kosmas, and Y. Chen, "A Q-slot monopole for UWB body centric wireless communications," *IEEE Transactions on Antennas and Propagation*, Vol. 65, No. 10, October 2017.
5. Bhattacharjee, S., M. Mitra, and S. R. Bhadra Chaudhuri, "An effective SAR reduction technique of a compact meander line antenna for wearable applications," *Progress In Electromagnetics Research M*, Vol. 55, 143–152, 2017.
6. Klemm, M. and G. Troester, "EM energy absorption in the human body Tissues due to UWB antennas," *Progress In Electromagnetics Research*, Vol. 62, 261–280, 2006.
7. Ray, K. P., "Design aspects of printed monopole antennas for ultra-wide band applications," *International Journal of Antennas and Propagation*, Vol. 2008, Article ID 713858, 8 pages, 2018.
8. Karthik, V. and T. Rama Rao, "Estimation of specific absorption rate using infrared thermography for the biocompatibility of wearable wireless devices," *Progress In Electromagnetics Research M*, Vol. 56, 101–109, 2017.
9. Karthik, V. and T. Rama Rao, "Thermal distribution based investigations on electromagnetic interactions with the human body for wearable wireless devices," *Progress In Electromagnetics Research M*, Vol. 50, 141–150, 2016.
10. Karthik, V. and T. Rama Rao, "SAR investigations on the exposure compliance of wearable wireless devices using infrared thermography," *Bioelectromagnetics*, Vol. 39, No. 6, 451–459, 2018.
11. Mohandoss, S., T. Rama Rao, B. N. Balarami Reddy, P. Sandeep Kumar, and M. Pushpalatha, "Fractal based ultra-wideband antenna development for wireless personal area communication applications," *International Journal of Electronics and Communications — (AEU)*, Vol. 93, 95–102, 2018.
12. Sanyal, R., A. Patra, P. Sarkar, and S Chowdhury, "Frequency and time domain analysis of a novel UWB antenna with dual band-notched characteristic," *International Journal of Microwave and Wireless Technology*, Vol. 9, No. 2, 427–436, 2017.

13. Zahrana, S. R., M. A. Abdallab, and A. Gaafar, "Time domain analysis for foldable thin UWB monopole antenna," *AEU — International Journal of Electronics and Communications*, 2018, https://doi.org/10.1016/j.aeue.2017.09.006.
14. "Revision of Part 15 of the commission's rules regarding ultra-wideband transmission systems. First report and order," *Technical Report ET Docket*, 98–153, FCC 02-48, Federal Communications Commission, 2002
15. "International Commission on Non-Ionizing Radiation Protection (ICNIRP). Guidelines for limiting exposure to time-varying electric, magnetic and electromagnetic fields (up to 300 GHz)," *Health Physics*, Vol. 74, 494–522, 1998.
16. Gabriel, C., "Compilation of the dielectric properties of body tissues at RF and microwave frequencies," Report N. AL/OE-TR-1996-0037, Occupational and environmental health directorate, Radiofrequency Radiation Division, Brooks Air Force Base, Texas, USA, June 1996.
17. Salim, M. and A. Pourziad, "A novel reconfigurable spiral-shaped monopole antenna for biomedical applications," *Progress In Electromagnetics Research Letters*, Vol. 57, 79–84, 2015.
18. Doddipalli, S., A. Kothari, and P. Peshwe, "A low profile ultrawide band monopole antenna for wearable applications," *International Journal of Antennas and Propagation*, Vol. 2017, Article ID 7362431, 9 pages, 2017.
19. Yeboah-Akowuah, B., P. Kosmas, and Y. Chen, "A Q-slot monopole for UWB body-centric wireless communication," *IEEE Transactions on Antennas and Propagation*, Vol. 65, No. 10, 5069–5075, 2017.
20. Bhattacharjee, S., M. Mitra, and S. R. Bhadra Chaudhuri, "An effective SAR reduction technique of a compact meander line antenna for wearable applications," *Progress In Electromagnetics Research M*, Vol. 55, 143–152, 2017.